Solution-Phase Processed Zinc Oxide Vertical Schottky Diode using Flow-limited Field-Injection Electrostatic Spraying

Riley Vesto[1], Matthew Pianfetti[1], Luke Hartmann[1], Rebekah Wilson[2], Hyungsoo Choi[1,3], Kyekyoon Kim[1,3,*]

[1]Department of Electrical and Computer Engineering, University of Illinois at Urbana-Champaign, Urbana, IL 61801, USA
[2]US Army Construction Engineering Research Laboratory, Champaign, Illinois 61826-9005, USA
[3]Holonyak Micro and Nanotechnology Laboratory, University of Illinois at Urbana-Champaign, Urbana, Illinois 61801, USA
*e-mail: kevinkim@illinois.edu, Phone: +1-(217) 333-7162

Keywords: ZnO, Schottky Diode, Solution Phase Processing, RF Power, Internet of Things

Abstract

All solution-phase processing of a proof-of-concept vertical Schottky diode was demonstrated, employing flow-limited field-injection electrostatic spraying with a total process time of < 2 hours at 290 ºC. Upon optimization, the present methodology would allow for cost-effective processing of rectifying and RF power conversion circuitry, enabling mass production of devices for Internet of Things applications.

INTRODUCTION

Internet of Things applications require massive distribution of low-profile sensors with the ability to wirelessly communicate and potentially transmit power. This is especially the case in industry and agricultural applications where the device needs are enormous [1]. As such rectifying and RF-power conversion circuitry needs cost-effective processing methods with high throughput.

Metal oxides are promising semiconducting materials for low-cost rectifying circuitry. They tend to be n-type with large bandgaps and electron mobilities and may be doped to directly control their conductivities [2]. The most common metal oxide platform is the In-Ga-Zn-O family of alloys due to their mobilities [3]. However, the inclusion of In and Ga can significantly increase the materials cost. Therefore, efforts have been made to produce diodes using ZnO alone at a small cost in performance. Another advantage to metal oxides is the ability to process materials in solution phase. In such processing, precursors in solution, applied to substrates, decompose or react, resulting in films of desired materials. Further, device fabrication without vacuum or high temperature processing would enable the use of inexpensive and often flexible polymer substrates [3].

Recently, high-performance ZnO RF Schottky diodes have been produced using a coplanar nanogap design [4, 5]. These diodes are impressive but require multiple steps alternating between metallization and solution processing to achieve the nanogap, lengthening the processing time and limiting the throughput. In addition, the reliance on vacuum processing for metallization limits the choice and size of substrates. Vacuum metallization is pervasive in the production of metal oxide Schottky diodes due to the reliance on distinct metals for asymmetric contacts [6].

In this work, we investigated the solution-phase processing of ZnO Schottky diode using flow-limited field-injection electrostatic spraying (FFESS).

METHODOLOGY

FFESS employs field-injection to charge precursor solutions, forming multiple jets that are broken into nanodrops of controlled sizes [7]. These drops conformally coat heated substrates, producing high-purity thin films of the desired material using metal-organic precursors [8]. The additional energy from Coulombic repulsion may allow for production of highly oriented crystalline materials at reduced temperatures [9,10]. The ability to control the droplet size allows FFESS to produce dense films with controlled thicknesses. This was used to stack layers of Ag and Al-doped ZnO (Al:ZnO) with decreasing areas and produce a vertical Schottky diode. The vertical diode design provides an advantage to current density, allowing for higher power applications. However, the predominant advantage to the vertical design is that it allows for the minimization of the length between contacts by controlling the Al:ZnO layer thickness without nano-scale patterning or self-assembled monolayers.

The Al:ZnO solution-phase precursors were prepared by dissolving equimolar amounts of zinc acetate and ethanolamine in 2-propanol, to which a solution of zinc acetate and aluminum acetylacetonate in ethanol with a molar ratio 3:1 of Zn:Al, refluxed for 2 hr, was added as desired. The Al:ZnO depositions were carried out using an 18 µl/min flowrate and 22 kV charging voltage. For the metal contacts, highly conductive Ag may be deposited directly from solution, enabling all solution-phase deposition. This was performed using a solution-phase precursor consisting of 0.2 M silver (I) 2-[2-(2-methoxyethoxy)ethoxy]acetate in ethanol with a 30 µl/min flowrate and 20 kV charging voltage.

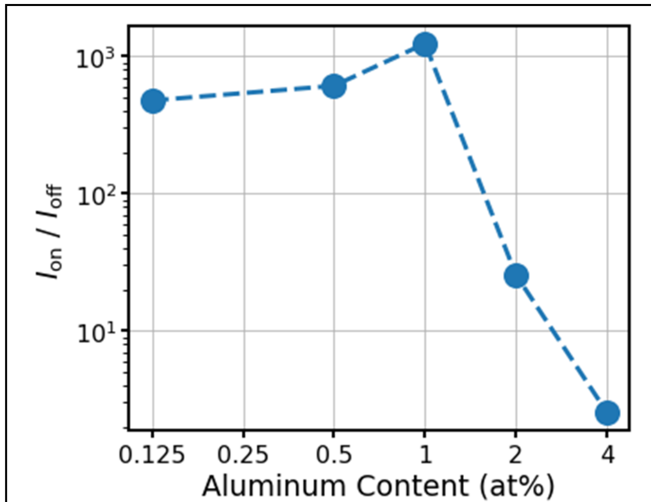

Fig. 1. I(2V) / I(-2V) ratio of forward and reverse bias currents for Ag-to-AZO interface measured by contacting both films with tungsten probes.

To achieve asymmetric operation of the diode, two Al:ZnO layers were deposited, one with 0.25 at% Al doping on the bottom and the other 4 at% Al doping on the top. The doping of the bottom layer was chosen to maximize conductivity while forming a Schottky contact with the Ag, whereas the doping of the top layer was chosen to promote tunneling current through the Ag-to-ZnO barrier. Fig. 1 demonstrates this behavior by comparing the I(2V)/I(-2V), labeled I_{on}/I_{off}, against Al:ZnO doping for a double layer Al:ZnO-on-Ag structure, with both films contacted using tungsten probes. Up to 1 at% Al, the current ratio increases due to the higher Al:ZnO conductivity allowing for higher forward current. Above 1 at% Al, the reverse bias tunneling current increases, causing the ratio to approach unity at 4 at% Al. The latter

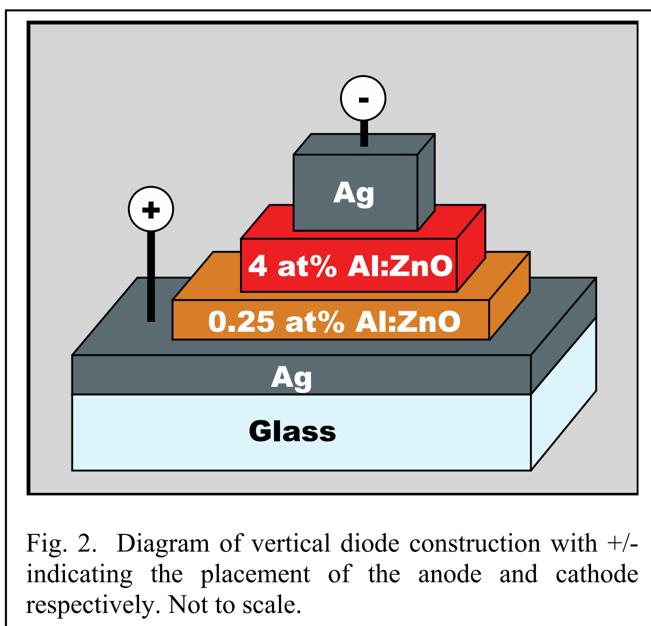

Fig. 2. Diagram of vertical diode construction with +/- indicating the placement of the anode and cathode respectively. Not to scale.

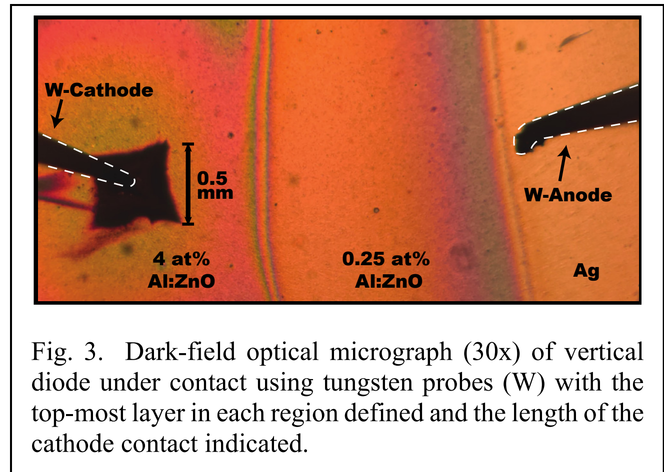

Fig. 3. Dark-field optical micrograph (30x) of vertical diode under contact using tungsten probes (W) with the top-most layer in each region defined and the length of the cathode contact indicated.

allows for the construction of the non-rectifying contact in our design.

The proof-of-concept diode was produced by successive depositions of 15 min Ag, 0.25 at% Al:ZnO, and 4 at% Al:ZnO layers onto a glass coverslip substrate at 290 ºC, with decreasing deposition areas defined using a Kapton tape shadow mask. After maintaining the substrate at 290 ºC for 45 min to remove any incorporated hydrogen from the Al:ZnO, which has been predicted to have a Fermi-level pinning effect [11]. Finally, a 15 min deposition of Ag was performed to construct the cathode. Fig. 2 shows a diagram of the final diode structure with the nesting layers and the placement of the anode and cathode probes indicated.

Results

An optical micrograph of the Schottky diode under contact with tungsten probes is shown in Fig. 3, demonstrating that the final Ag layer which defines the working area of the device to be $0.5 \times 0.5\ mm^2$. Despite the simplicity of the shadow-masking approach, well defined features are easily produced. Scanning electron micrographs of the diode cross-section are shown in Fig. 4, demonstrating the respective film thicknesses. Each successive micrograph demonstrates a different region of the cross-section where the respective films are defined. The film thickness increases per layer due to the Kapton mask which focuses the charged nano-drop beam. This resulted in the topmost Ag to be 550 nm thick, protecting the diode from scratching during probing.

The current-vs-voltage curve of diode is demonstrated in Fig. 5. The ratio of the forward and reverse bias current was I(2V) / I(-2V) = 4.03 µA / 171 nA = 23.6. This demonstration of rectification indicates the promise for the technology. Further improvement may be achieved by increasing the forward current. This may be achieved by increasing the doping of the first Al:ZnO layer, increasing the cathode area, or decreasing the Al:ZnO thicknesses.

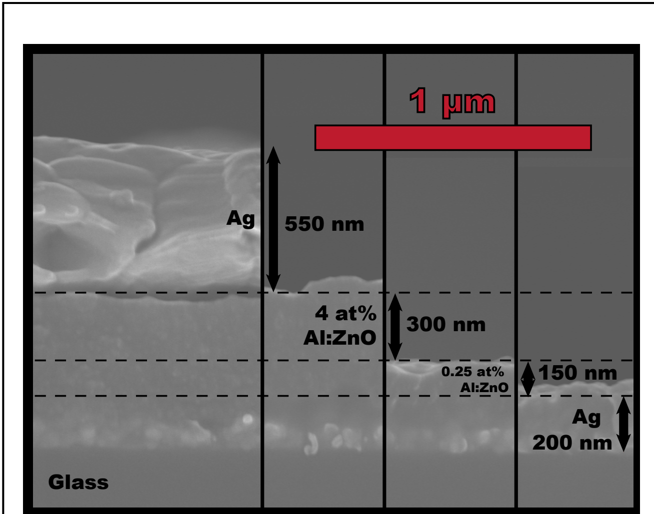

Fig. 4. Scanning electron micrographs of the diode cross-section, all at the same magnification with the top of the substrate aligned. Each successive image demonstrates a different region of the device where the respective films are defined.

For further characterization of the diodes, the plotting methods of Cheung et al. were employed [12]. This was accomplished by noting, based on the Schottky diode equation:

$$\frac{dV}{d(\ln I)} = \frac{nk_BT}{q} + IR_s,$$

where R_s is the series resistance of the diode, n the ideality factor, q the electron charge, and k_BT = 25.7 meV the room temperature thermal energy. The left-hand side was calculated using central differences and plotted on the right-axis in Fig. 6. By linear regression, we obtain R_s = 220 kΩ and n = 7.61. The series resistance is larger than desired which indicates the limiting factor of the forward current. The ideality is large, seemingly limited by recombination due to traps at the Ag-to-Al:ZnO interface. This may be improved with maturity of the technology.

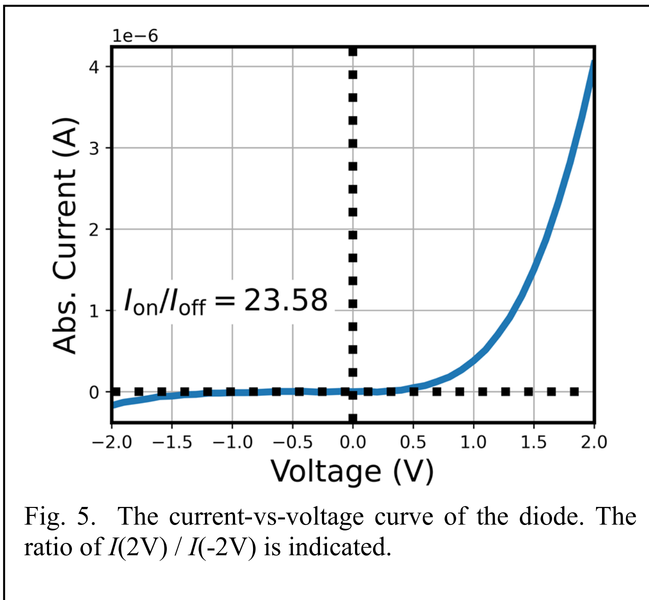

Fig. 5. The current-vs-voltage curve of the diode. The ratio of I(2V) / I(-2V) is indicated.

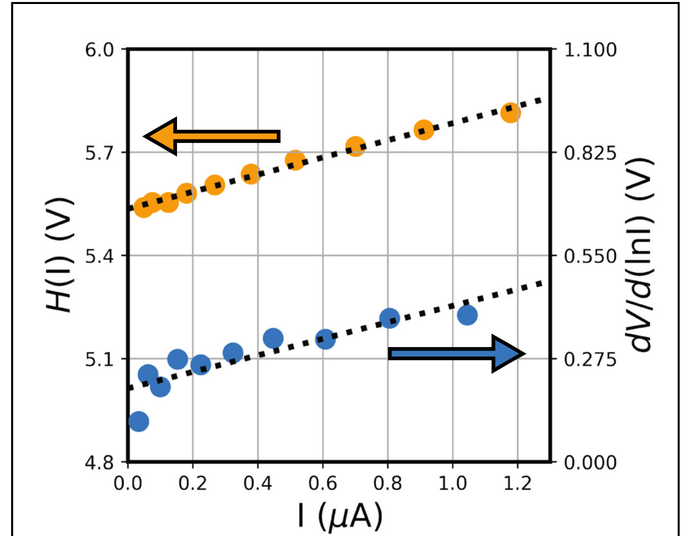

Fig. 6. Cheung plots used for extraction of the diode parameters. Linear regression fits yield R_s = 220 kΩ, n = 7.61, and ϕ_b = 0.727 V.

The barrier height, ϕ_b, may be calculated by noting:

$$H(I) \equiv V - \frac{nk_BT}{q}\ln\frac{I}{A^*A_{eff}T^2} = n\phi_b + IR_s,$$

where A^* is Richardson's constant, taken to be 8.6 A/cm^{2}K^2, and A_{eff} the effective area of the diode, assumed to be the area of the anode. This function is plotted on the right-axis of Fig 6. By linear regression, we obtain R_s = 249 kΩ and ϕ_b = 0.727 V. The second fit to the R_s is within a margin to the first fit. The barrier height is within a margin to the difference in expected work functions of the silver and ZnO. This large barrier height will allow for further reduction in reverse bias current in future diodes by limiting leakage current due to processing defects.

Conclusions

A prototype Schottky diode was produced entirely from solution using FFESS by employing a Kapton-tape shadow-masking approach. The resultant device performance is preliminary but shows promise towards eventual use in power conversion for large-scale internet of things applications. Further improvements may be achieved by adjusting the Al:ZnO layer thicknesses and doping, as well as improving the processing to ensure a clean Ag-to-Al:ZnO interface. Additionally, precursor modifications may allow materials deposition at temperatures below 200 °C, allowing for processing of diodes on flexible and inexpensive polymers. Because this processing does not rely on vacuum processing and uses relatively few precursor materials, the diode can be cost-effective. Further, the full processing, starting from the substrate, can be performed in less than 2 hr, allowing for mass production of the diode and circuitry. Rapid and

accessible processing techniques, such as these, will be necessary for future integrated circuits to reach the scales required for distributed sensing applications.

Acknowledgements

This work was financially supported by the U.S. Army CERL, Grant No. W9132T18C0010, and the Kim-Fund of the University of Illinois, Grant No. UIUC-933008-633134. R.V. gratefully acknowledges the Bardeen Fellowship and the ECE Distinguished Fellowship of the University. The materials characterization work was carried out in part in the Materials Research Laboratory Central Research Facilities. Helpful discussions with Frank Kelly and Matthew Landi are greatly appreciated.

References

[1] E. Sisinni *et al*, *IEEE Trans. Ind. Inf.*, vol. 14, no. 11, pp. 4724–4734, Nov. 2018

[2] T. Minami, *Semicond. Sci. Technol.*, vol. 20, no. 4, pp. S35–S44, Apr. 2005

[3] L. Petti *et al.*, *Applied Physics Reviews*, vol. 3, no. 2, p. 021303, Jun. 2016

[4] J. Semple *et al.*, *Small*, vol. 12, no. 15, pp. 1993–2000, Apr. 2016

[5] D. G. Georgiadou *et al.*, *Nat Electron*, vol. 3, no. 11, pp. 718–725, Nov. 2020

[6] J. Semple, *ACS Appl. Mater. Interfaces*, vol. 8, no. 35, pp. 23167–23174, Sep. 2016

[7] W. Gu *et al.*, *Appl. Phys. Lett.*, vol. 87, no. 8, p. 084107, Aug. 2005

[8] K. Kim and C. K. Ryu, *Nanostructured Materials*, vol. 4, no. 5, pp. 597–602, Sep. 1994

[9] S. H. Rhee *et al.*, *Thin Solid Films*, vol. 396, no. 1–2, pp. 23–28, Sep. 2001

[10] R. E. Vesto *et al.*, *AIP Advances*, vol. 10, no. 9, p. 095211, Sep. 2020

[11] H. H. Nahm *et al.*, *Sci. Rep.*, vol 4, p. 4124, Feb. 2014

[12] S. K. Cheung and N. W. Cheung, *Appl. Phys. Lett.*, vol. 49, No. 85, pp. 85-87, May 1986